Journal of Sound and Vibration (1999) **227**(2), 427–447
Article No. jsvi.1999.2353, available online at http://www.idealibrary.com on IDEAL®

EXCITATION OF VIBRO-IMPACT SYSTEMS BY PERIODIC IMPULSES

S. A. KEMBER AND V. I. BABITSKY

*Department of Mechanical Engineering, Loughborough University, Loughborough, Leicestershire, LE*11 3*TU, England*

(*Received* 7 *August* 1998, *and in final form* 30 *April* 1999)

Linear mechanical systems with periodic impulse excitation are related to the classical area of dynamical analysis. The exact solutions obtained played an important role in mathematics and had numerous applications in vibration analysis and machine dynamics. The introduction of non-linear factors into the excited models makes integration impossible and generally involves the use of various difficult estimated approximations. However, it is shown here that for one important class of strongly non-linear mechanical systems, vibro-impact systems, it is possible to produce an exact steady state solution of the problem of periodic impulse excitation by the use of the periodic Green function method. These solutions can be applied to the analysis of impulse transformations in percussion machines, non-linear mechanical structures and in systems of vibration protection.

1. INTRODUCTION

Linear mechanical system excited by periodic impulses represent the simplest model of the influence of periodic impacts on mechanical systems. The explicit finite form of the exact solutions in these cases [1] allows the accumulative effect of repeated impacts on the development of oscillations to be studied. The problem of periodic impulse excitation in mechanical systems, however, often demands the introduction of a non-linear factor into the model in the form of various types of contact interaction. The interest with respect to the effects of multiple impact interactions inspired the development of the theory of vibro-impact systems, an important area of non-linear mechanical analysis, which has many applications in engineering.

A method commonly used to study a vibro-impact system involves the simultaneous solution of a series of equations, which include the general solutions of the differential equations of motion in between impacts, and conditions of periodicity and impact for one particular cycle of motion. This method is used to find a steady state periodic behaviour and transients are ignored. It was first used in vibro-impact studies by Rusakov and Kharkevich [2] and is known as the *stitching method*. It was shown later that an analysis of solution stability under small perturbations can be performed in this case with the help of linear difference

0022-460X/99/420427 + 21 $30.00/0

equations [3]. The method as a whole has a clear geometrical interpretation with the help of Poincaré mappings [4, 5].

The analysis of periodic solutions with the stitching method tends to be cumbersome and so is limited in application to the simplest models of structures and excitations. Often the number and complexity of the equations are such that numerical solution is required. Moreover, the necessity of using the general solutions of differential equations for describing the motion in between the impacts makes the whole method inapplicable when such general integrals are absent or when a mathematical description of the model is incomplete.

These problems were overcome with the development of methods based on the structural description of mechanical systems [5]. These included both the use of traditional methods of approximate non-linear analysis with the help of equivalent (harmonic and stochastic) linearization, and the development of a new analytical technique making use of *periodic Green functions* (PGF) [5, 6]. The latter were previously introduced into general non-linear analysis as *impulse-frequency characteristics* [7, 8]. It has been shown [5] that, in integrable cases, the PGF method is able to analyze many complex systems without resorting to numerical solutions. The PGF method generalized the previous approaches to vibro-impact interaction modelling by a series of Dirac δ functions [9, 10] and introduced an effective application of integral equations, as well as asymptotic, frequency, and structural concepts into vibro-import analysis. An English edition of reference [5] contains extensive updated bibliography on vibro-impact dynamics.

The development of the PGF method opened up a wide variety of new applications in the analysis and optimizing of vibro-impact systems [11, 12]. It permitted the solution of problems with parametric excitation [11], and distributed structural and impact elements [11, 13]. The PGF provided a natural method for the analysis of regular and random perturbations of periodical vibro-impact motions with the use of an averaging technique [11, 12], for solution to the problem of optimal control of such motions [12].

In the current study the PGF method is applied to the analysis of the transformation of periodic impulsive excitation by a vibro-impact system. This has several applications in percussion machines and in the vibration analysis of mechanical structures.

2. FORMULATION OF THE PROBLEM AND ITS SOLUTION BY THE PGF METHOD

The model analyzed in this paper is shown in Figure 1. Two arbitrary single-degree-of-freedom damped systems have a periodic one-dimensional impact interaction between them under a periodic impulse excitation $f(t)$ with impulses by magnitude F applied to one of the systems. The systems have an initial distance Δ between the two masses when there is no excitation. If Δ is negative then the masses are initially in contact with a preload. The parameters of the excited (active) system are identified by the index 1, and those of the second (passive) system by the index 2. Each system has a mass m, a linear spring with spring constant k, and

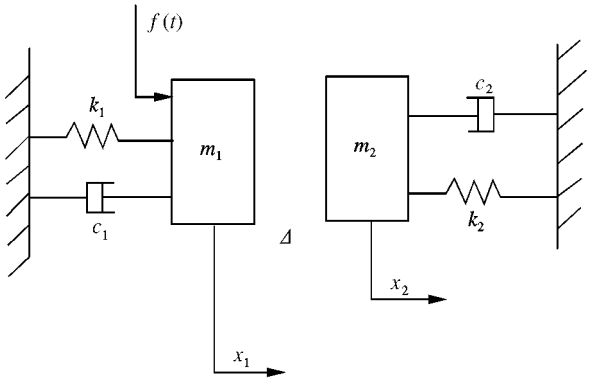

Figure 1. The two-degree-of-freedom system.

a linear damper with damping coefficient c. The directions of positive displacements x are indicated in Figure 1.

A similar structure under *sinusoidal* excitation has been analyzed previously with simplifications in references [3, 9, 14–17]. The used cumbersome technique did not permit the authors to reveal entirely the resonant behaviour of the system. In this work, we demonstrate also, as an example, a simple solution of this problem in explicit finite form with PGF method and proper frequency responses of the system.

The investigation here is limited to the analysis of forced vibration for which the frequency of internal impacts is the same as the frequency of the externally applied impulses. Other patterns of periodic vibro-impact regimes like sub- and super-periodic resonances can be similarly analyzed.

The displacement x_1 of mass m_1 in the operating regime of interest can be represented as the sum of two components: the response to the impulsive excitation, and the response to the impact interaction with mass m_2. The steady state response to the impact with mass m_2 is the PGF given in equation (A6) multiplied by the unknown impulse of interaction J between the two masses. An impact between the two masses occurs at $t = \gamma T$ where T is the period of the excitation, $\gamma = 0, 1, 2, \ldots$ The response is $J\chi_1(t)$ where χ_1 is the PGF of the single-degree-of-freedom system containing m_1 and where J is the impulse acting on m_1. Here $J \geqslant 0$.

The steady state response to the impulsive excitation is similarly formed from the impulse F and the PGF. As the impact excitation does not occur at the same time as the impact between the two masses, a PGF with a time lead is used. This is developed by using the transformation in equation (A7). The response is $F\chi_1(t + \tau)$.

As the mass–spring–damper system is linear, the two responses can be added to give the equation of motion of m_1:

$$x_1(t) = F\chi_1(t + \tau) - J\chi_1(t). \tag{1}$$

Likewise the equation of motion for m_2 is

$$x_2(t) = J\chi_2(t), \tag{2}$$

where the PGFs (see the appendix) are

$$\chi_1(t) = \frac{e^{-b_1 t}}{m_1 \lambda_1}\left(\frac{\sin \lambda_1 t + e^{-b_1 T}\sin \lambda_1 (T - t)}{1 + e^{-2b_1 T} - 2e^{-b_1 T}\cos \lambda_1 T}\right)$$

and

$$\chi_1(t + \tau) = \frac{e^{-b_1(t+\tau-T)}}{m_1 \lambda_1}\left(\frac{\sin \lambda_1 (t + \tau - T) + e^{-b_1 T}\sin \lambda_1 (2T - t - \tau)}{1 + e^{-2b_1 T} - 2e^{-b_1 T}\cos \lambda_1 T}\right)$$

when $0 < t < T$ and $T < t + \tau < 2T$

or

$$\chi_2(t + \tau) = \frac{e^{-b_2(t+\tau)}}{m_1 \lambda_1}\left(\frac{\sin \lambda_1 (t + \tau) + e^{-b_1 T}\sin \lambda_1 (T - t - \tau)}{1 + e^{-2b_1 T} - 2e^{-b_1 T}\cos \lambda_1 T}\right)$$

when $0 < t < T$ and $0 < t + \tau < T$ and

$$\chi_2(t) = \frac{e^{-b_2 t}}{m_2 \lambda_2}\left(\frac{\sin \lambda_2 t + e^{-b_2 T}\sin \lambda_2 (T - t)}{1 + e^{-2b_2 T} - 2e^{-b_1 T}\cos \lambda_2 T}\right),$$

where the following relationships apply to both systems (with appropriate subscripts):

$$2b = 2\Omega\zeta = c/m, \qquad \lambda = \sqrt{\Omega^2 - b^2}, \qquad \Omega^2 = k/m, \qquad \zeta = c/2\sqrt{km}$$

and Ω is the undamped natural frequency of the first mode and ζ is the damping ratio.

The PGFs can be simplified. Let

$$B_1 = e^{-b_1 T}, \qquad B_2 = e^{-b_2 T}, \qquad A_1 = 1/m_1 \lambda_1 (1 + B_1^2 - 2B_1 \cos \lambda_1 T)$$

and

$$A_2 = 1/m_2 \lambda_2 (1 + B_2^2 - 2B_2 \cos \lambda_2 T).$$

If one assumes that the motion of the system has reached a steady state with all displacements having the same period T, and that at $t = 0$, impact between m_1 and m_2 occurs, the two displacements at $t = 0$ can be related by

$$x_1(0) - x_2(0) = \Delta. \tag{3}$$

There is another relationship at $t = 0$ which is the equation relating J to velocity. This can be calculated from the following three equations.

The equation for conservation of momentum,

$$m_1 \dot{x}_{1+} + m_2 \dot{x}_{2+} = m_1 \dot{x}_{1-} + m_2 \dot{x}_{2-} \tag{4}$$

(where subscript + indicates the velocity after impact and subscript − the velocity before impact); the definition of the coefficient of restriction R

$$R = (\dot{x}_{2+} - \dot{x}_{1+})/(\dot{x}_{1-} - \dot{x}_{2-}), \tag{5}$$

and the impulse–momentum relationship:

$$J = (m_2\dot{x}_{2+} - m_2\dot{x}_{2-}). \tag{6}$$

Relationships (4)–(6) can be arranged to give

$$J = M(1 + R)(\dot{x}_{1-} - \dot{x}_{2-}), \tag{7}$$

where $M = m_1m_2/(m_1 + m_2)$.

So at $t = 0$, the displacement of the active system is

$$x_1(0) = FA_1e^{-b_1\tau}(\sin\lambda_1\tau + B_1\sin\lambda_1(T - \tau)) - J\chi_1(0) \tag{8}$$

and the displacement of the passive system is

$$x_2(0) = J\chi_2(0), \tag{9}$$

where $\chi_1(0) = A_1B_1\sin\lambda_1T$ and $\chi_2(0) = A_2B_2\sin\lambda_2T$.

Hence substituting equations (8) and (9) into equation (3) yields

$$\Delta = FA_1e^{-b_1\tau}(\sin\lambda_1\tau + B_1\sin\lambda_1(T - \tau)) - J\chi, \tag{10}$$

where $\chi = \chi_1(0) + \chi_2(0)$.

At $t = 0$, the velocities are

$$\begin{aligned}\dot{x}_{1-}(0) = {} & FA_1e^{-b_1\tau}(\lambda_1\cos\lambda_1\tau - b_1\sin\lambda_1\tau) \\ & - FA_1B_1e^{-b_1\tau}(\lambda_1\cos\lambda_1(T - \tau) + b_1\sin\lambda_1(T - \tau)) - J\dot{\chi}_{1-}(0)\end{aligned} \tag{11}$$

and

$$\dot{x}_{2-}(0) = J\dot{\chi}_{2-}(0), \tag{12}$$

where $\dot{\chi}_{1-}(0) = \dot{\chi}_1(T) = A_1B_1(\lambda_1\cos\lambda_1T - b_1\sin\lambda_1T) - A_1B_1^2\lambda_1$ and $\dot{\chi}_{2-}(0) = \dot{\chi}_2(T) = A_2B_2(\lambda_2\cos\lambda_2T - b_2\sin\lambda_2T) - A_2B_2^2\lambda_2$.

Inserting equations (11) and (12) into equation (7) gives

$$\begin{aligned}J = {} & M(1 + R)FA_1e^{-b_1\tau}(\lambda_1\cos\lambda_1\tau - b_1\sin\lambda_1\tau) \\ & - M(1 + R)FA_1B_1e^{-b_1\tau}(\lambda_1\cos\lambda_1(T - \tau) + b_1\sin\lambda_1(T - \tau)) \\ & - M(1 + R)J\dot{\chi},\end{aligned} \tag{13}$$

where $\dot{\chi} = \dot{\chi}_1(T) + \dot{\chi}_2(T)$.

The two simultanious equations (10) and (13) contain two unknowns, J and τ which need to be determined. As the two equations are very complex, they can be simplified if it is assumed that the damping coefficient c_1 is small and the damping losses are very low in value in comparison with the impact losses (as usual in real mechanical systems). As b_1 is calculated by dividing c_1 by $2m_1$, so b_1 will be close to zero. Thus the following simplifications can be made:

$$e^{-b_1\tau} \approx 1, \quad \lambda_1 = \sqrt{\Omega_1^2 - b_1^2} \approx \Omega_1, \quad B_1 = e^{-b_1T} \approx 1$$

and

$$A_1 = 1/m_1\lambda_1(1 + B_1^2 - 2B_1\cos\lambda_1 T) \approx 1/m_1\Omega_1(2 - 2\cos\Omega_1 T),$$

so equations (10) and (13) become

$$(\Delta + J\chi)/FA_1 = \sin\Omega_1\tau + \sin\Omega_1(T - \tau) \tag{14}$$

and

$$J(1/M(1 + R) + \dot{\chi})/FA_1\Omega_1 = \cos\Omega_1\tau - \cos\Omega_1(T - \tau). \tag{15}$$

If equations (14) and (15) are squared and added, the terms with the time lead τ are removed. The result can be rearranged to produce

$$J = \chi\Delta\Omega_1^2/(1/M(1 + R) + \dot{\chi})^2 + \Omega_1^2\chi^2$$
$$\times\left(-1 \pm \sqrt{1 - \frac{((1/\mathrm{M}(1 + R) + \dot{\chi})^2 + \Omega_1^2\chi^2)(\Delta^2 - 2rF^2A_1^2)}{\chi^2\Delta^2\Omega_1^2}}\right), \tag{16}$$

where $r = 1\text{-}\cos\Omega_1 T$.

The time lead τ can be found by solving equations (14) and (15) for $\sin\Omega_1\tau$ and $\cos\Omega_1\tau$ to give the following:

$$\sin\Omega_1\tau = \frac{r\Omega_1(\Delta + J\chi) - J(1/M(1 + R) + \dot{\chi})\sin\Omega_1 T}{2rFA_1\Omega_1}, \tag{17}$$

$$\cos\Omega_1\tau = \frac{\Omega_1(\Delta + J\chi)\sin\Omega_1 T + rJ(1/M(1 + R) + \dot{\chi})}{2rFA_1\Omega_1}, \tag{18}$$

Equation (16) for J is similar to the result obtained for an identical system with sinusoidal excitation of $F_0\cos\omega t$. The equation of motion for the active system becomes

$$x_1(t) = A\cos(\omega t + \varphi) - J\chi_1,$$

where $A = F_0/\sqrt{(k_1 - m_1\omega^2)^2 + (c_1\omega)^2}$. The method is identical to that used for the impulse excitation so that two equations are found:

$$\frac{\Delta + J\chi}{A} = \cos\varphi \quad \text{and} \quad \frac{-J(1/M(1 + R) + \dot{\chi})}{A\omega} = \sin\varphi,$$

These can be solved to give the result

$$J = \chi\Delta\omega^2/(1/M(1 + R) + \dot{\chi})^2 + \omega^2\chi^2$$
$$\times\left(-1 \pm \sqrt{1 - \frac{((1/M(1 + R) + \dot{\chi})^2 + \omega^2\chi^2)(\Delta^2 - A^2)}{\chi^2\Delta^2\omega^2}}\right), \tag{19}$$

Solution (19) is similar to the solution obtained for a generalized system with sinusoidal excitation given in reference [5].

3. STABILITY OF THE SOLUTION

Equation (16) has two solutions for J, one with a positive square root and one with a negative square root. The method used here to find the stable solution is the energy balance principle, as explained in references [5].

If all the energies existing in a stationary system are summed over one period, some of those energies will not sum to zero. These are the energy applied to the system by the excitation and the energy lost through dissipation. In a stationary regime these two energies will balance each other. But if such a system receives a perturbation, then the energy balance is lost. However, if the system is stable then the energies of the transient will be arranged in such a way that the system will return to its stationary behaviour.

Based on the previous works with sinusoidally excited systems [5, 11], it is proposed that equation (17) represents the energy balance of the system with $\sin \Omega_1 \tau$ proportional to the energy from the excitation. It has not been possible to prove this rigorously, at this stage. However, this assumption is supported by the results presented in the following sections.

Define a, q, h, *and* d as follows:

$$a = -\frac{r\Omega_1 \Delta}{2rFA_1\Omega_1}, \qquad q = \frac{-(r\Omega_1\chi - (1/M(1+R) + \dot{\chi})\sin \Omega_1 T)}{2rFA_1\Omega_1}$$

$$h = \frac{\Omega_1 \Delta \sin \Omega_1 T}{2rFA_1\Omega_1}, \qquad d = \frac{\Omega_1 \chi \sin \Omega_1 T + r(1/M(1+R) + \dot{\chi})}{2rFA_1\Omega_1}, \tag{20}$$

so that equations (17) and (18) can be rewritten as

$$\sin \Omega_1 \tau = \sin \varphi = -(a + qJ) \quad \text{and} \quad \cos \Omega_1 \tau = \cos \varphi = h + dJ. \tag{21, 22}$$

It is proposed that after a small perturbation the motion becomes

$$\tilde{x}_1(t) = F\chi_1(t + \tilde{\tau}(t)) - \tilde{J}(t)\chi_1(t),$$

where $\tilde{\varphi}(t) = \Omega_1 \tilde{\tau}(t)$ and $\tilde{\varphi}(t)$ and $\tilde{J}(t)$ are arbitrary slowly varying variables. So as equation (21) represents the energy balance and $\sin \varphi$ is proportional to the energy of excitation, then the system is stable if the following condition is true:

$$\frac{\mathrm{d}}{\mathrm{d}\tilde{J}}[a + q\tilde{J} + \sin \tilde{\varphi}]_{\tilde{J}=J} > 0. \tag{23}$$

This means that under the perturbation the balance of energies changes in such a manner as to compensate the perturbation.

Differentiating equation (23) gives

$$\{q + \cos \tilde{\varphi}(\mathrm{d}\tilde{\varphi}/\mathrm{d}\tilde{J})\}_{\tilde{J}=J} > 0, \tag{24}$$

this introduction $\tilde{\varphi}$ and $\tilde{J}$ as two arbitrary functions which can be connected by an additional condition. Here it is convenient to take this additional condition to be equation (22). Inserting the two arbitrary functions into equation (22) and

differentiating gives

$$-\sin\tilde{\varphi}\,(\mathrm{d}\tilde{\varphi}/\mathrm{d}\tilde{J}) = d. \tag{25}$$

Upon using equation (25) to substitute for $\mathrm{d}\tilde{\varphi}/\mathrm{d}\tilde{J}$, equation (24) becomes

$$\{q - d\cot\tilde{\varphi}\}_{\tilde{J}=J} > 0, \tag{26}$$

when $\tilde{J} = J$ and $\tilde{\varphi} = \varphi$. If equation (22) is divided by equation (21) to give $\cot\varphi$, then equation (26) may be written as

$$(hd + d^2J)/(a + qJ) + q > 0. \tag{27}$$

Multiplying equation (27) by $a + qJ$ and rearranging yield,

$$J > -(aq + hd)/(q^2 + d^2). \tag{28}$$

Substituting for a, q, h and d from equation (20) then gives

$$J > -\chi\Delta\Omega_1^2/(1/M(1 + R) + \dot{\chi})^2 + \Omega_1^2\chi^2. \tag{29}$$

Therefore, the positive root of equation (16) corresponds to the stable solution. This agrees with the results for other vibro-impact systems [5, 11].

4. REDUCTION TO A SINGLE-DEGREE-OF-FREEDOM SYSTEM

Equation (16) can be simplified to show the underlying non-linear structure of the system. If c_2 is made very small and R almost 1, then $1/M(1 + R) + \dot{\chi} = 0$ so equation (16) simplifies to

$$J = -\frac{\Delta}{\chi} + \frac{FA_1\sqrt{2r}}{\chi}. \tag{30}$$

If m_2 is very large so that the system is effectively a single-degree-of-freedom system (an impact oscillator) then

$$\chi = A_1\sin\Omega_1 T = \frac{1}{2m_1\Omega_1\tan(\Omega_1 T/2)}$$

as $r = 1 - \cos\Omega_1 T = 2\sin^2(\Omega_1 T/2)$ and $\sin\Omega_1 T = 2\sin(\Omega_1 T/2)\cos(\Omega_1 T/2)$, so equation (30) becomes

$$J = -2m_1\Omega_1\Delta\tan(\Omega_1 T/2) + F/\cos(\Omega_1 T/2) \tag{31}$$

If the system is under free vibration ($F = 0$) then the result is identical to the result given in reference [11] for an impact oscillator, and the frequency characteristic (see Figure 2) is a typical backbone curve for a non-linear system. This shape is retained as long as the second term in equation (31) is small in comparison to the first term. Similarly the sinusoidal result (19) can be simplified to

$$J = -2m_1\Omega_1\Delta\tan(\Omega_1 T/2) + 2F_0\Omega_1\tan(\Omega_1 T/2)/\sqrt{(\Omega_1^2 - \omega^2)^2}. \tag{32}$$

Again the same backbone curve is in the first term of the equation.

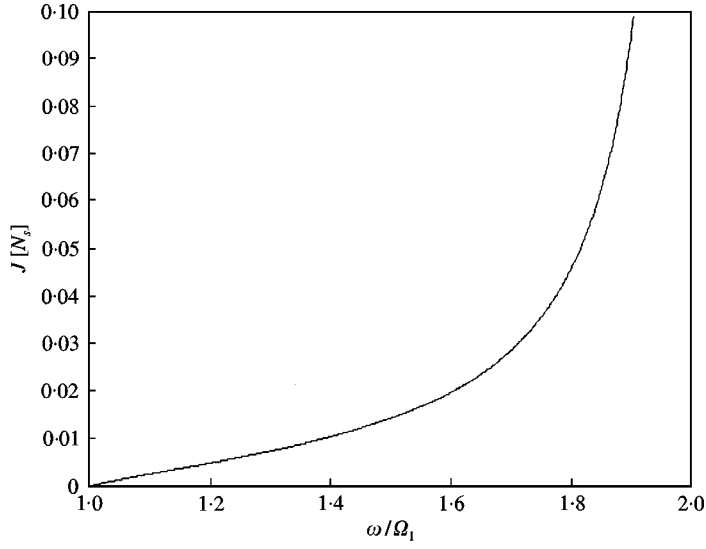

Figure 2. The backbone curve derived from equation (31).

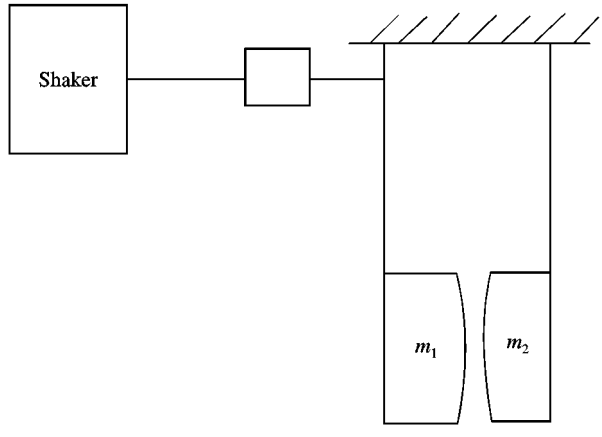

Figure 3. Experimental model.

5. APPLICATION TO A REALISTIC PHYSICAL SYSTEM

The physical parameters of a working laboratory model (see Figure 3) similar to that used for the PGF model (Figure 1), were used to study the behaviour of a realistic physical system. The laboratory model, when excited sinusoidally, was observed to have two resonances, one at 5·6 Hz and the other at 9 Hz. The resonance at the lower frequency was 'linear' in form, as the frequency of resonance was unaffected by changes in the excitation amplitude. The displacements of the two masses were large and the masses moved together in the same direction with a weak contact—a *grazing resonance*. At the higher natural frequency the two masses moved in opposite directions with one strong impact per cycle—a *clapping*

resonance. This clapping resonance was strongly affected by changes in excitation amplitude, demonstrating non-linear features. In addition, when the frequency of excitation was swept up through the resonances, both resonances occurred, while on the downsweep only the first resonance occurred. Based on this experiment, the following parameters were chosen as inputs to the PGF model; $m_1 = 0{\cdot}125\,\text{kg}$, $m_2 = 0{\cdot}094\,\text{kg}$, $k_1 = 135\,\text{N/m}$, $k_2 = 128\,\text{N/m}$, $c_1 = c_2 = 0\,\text{Ns/m}$, $R = 0{\cdot}7$ and $\Delta = 0{\cdot}001\,\text{m}$.

The response of the PGF model to a range of sinusoidal excitation frequencies is shown in Figure 4, and the equivalent response for impulse excitation is shown in Figure 5. The solid lines indicate the displacement behaviour for the active system and the dotted lines represent the passive system. The displacements were calculated for each excitation frequency and the magnitude of the peak amplitude as a half of the total swing is plotted.

The first peak at $\omega/\Omega_1 = 1{\cdot}05$ (5·5 Hz) is almost identical for both types of excitation and for both active and passive systems. The displacement graph for impact excitation (Figure 6) shows this resonance to be a grazing resonance.

The second peak is at $\omega/\Omega_1 = 2{\cdot}13$ (11·1 Hz). From the displacement graph (Figure 7) the behaviour shown by the model is the clapping resonance. The behaviour under sinusoidal excitation at both resonances is identical apart from the amplitudes, The result correlates well with the laboratory model behaviour. However, the amplitudes are likely to be different as the excitation amplitude varied during the experiment. The response of the system in grazing resonance has a strong amplification because viscous damping, which affects strongly this

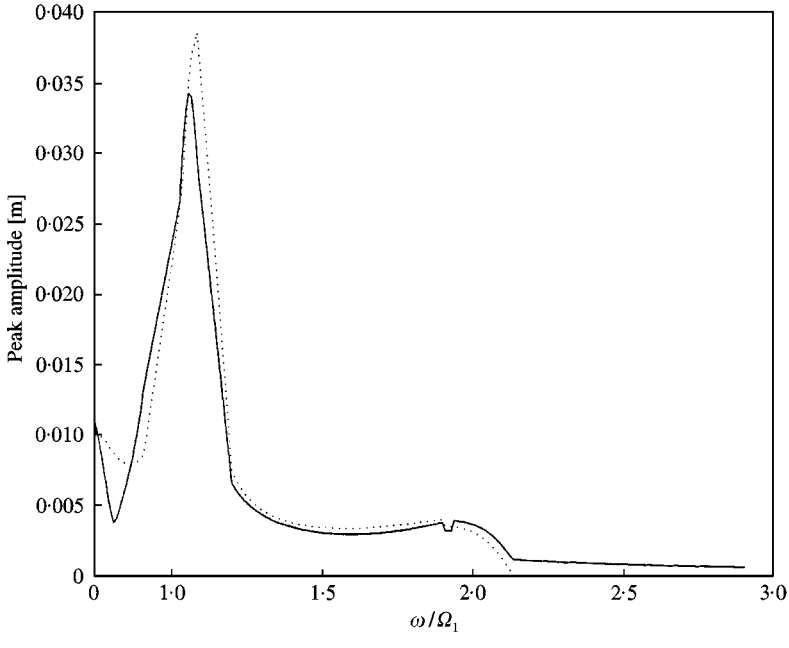

Figure 4. Frequency response to sinusoidal excitation. The active system displacements have the solid line and the passive system the broken line.

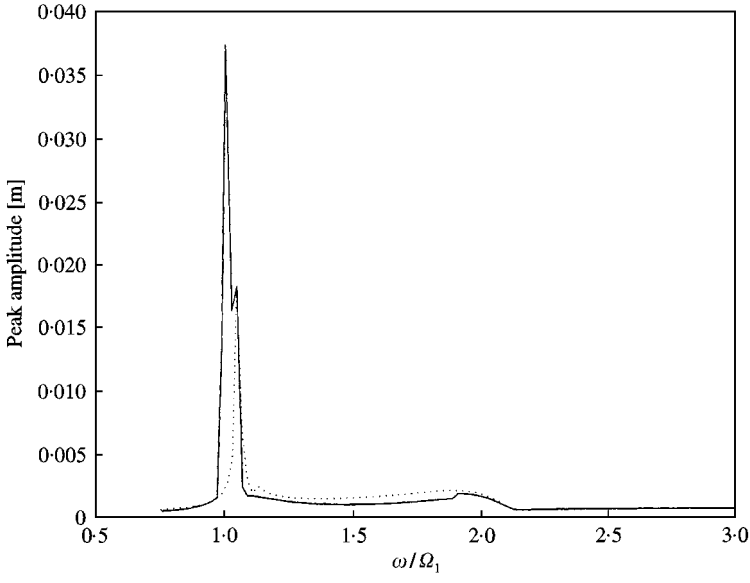

Figure 5. Frequency response to impact excitation.

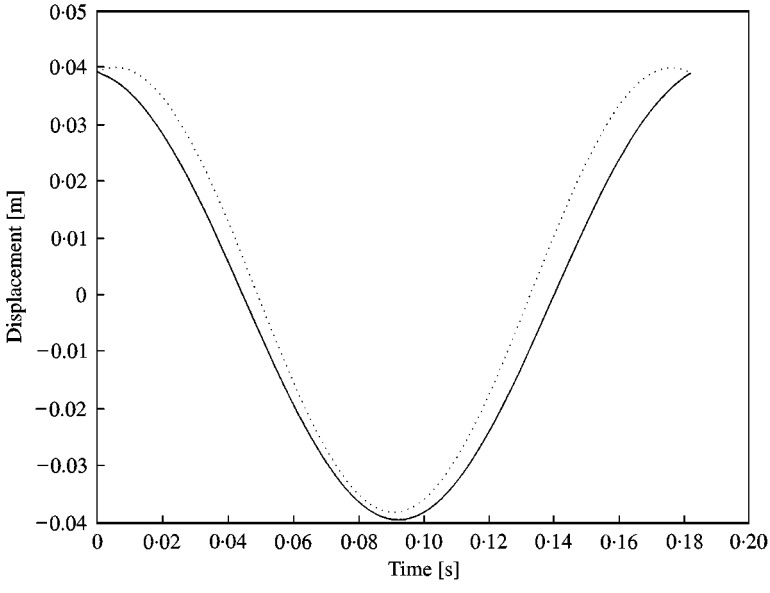

Figure 6. Behaviour over one period at $\omega/\Omega_1 = 1{\cdot}05$ (5·5 Hz) impact excitation.

resonance, was not applied in calculations. The clapping resonance is controlled mainly by impact damping. With an increase of R it comes more prominant. The graph of J against frequency during the clapping resonance follows to the backbond curve shown in Figure 3. The results for the two types of excitation were identical, so only one is shown in this paper (see Figure 8).

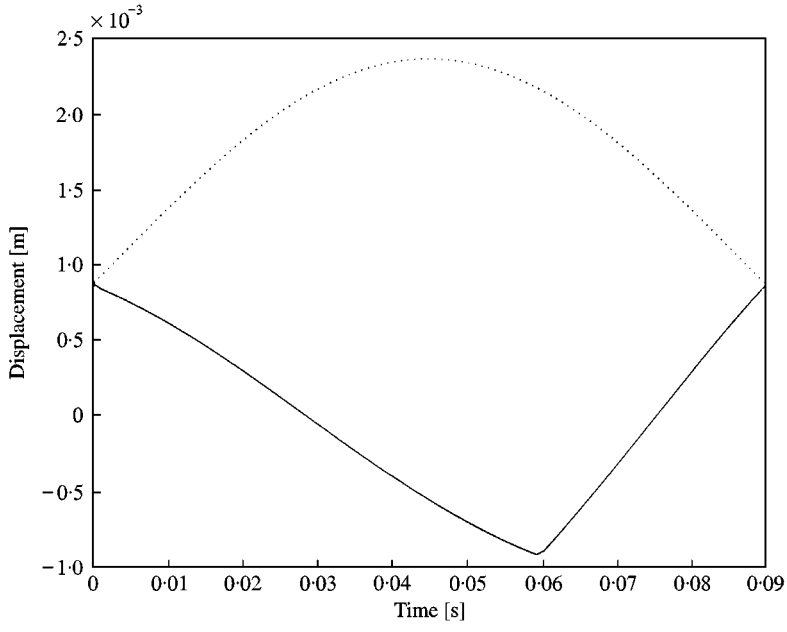

Figure 7. Behaviour over one period at $\omega/\Omega_1 = 2{\cdot}13$ (11·1 Hz) impact excitation.

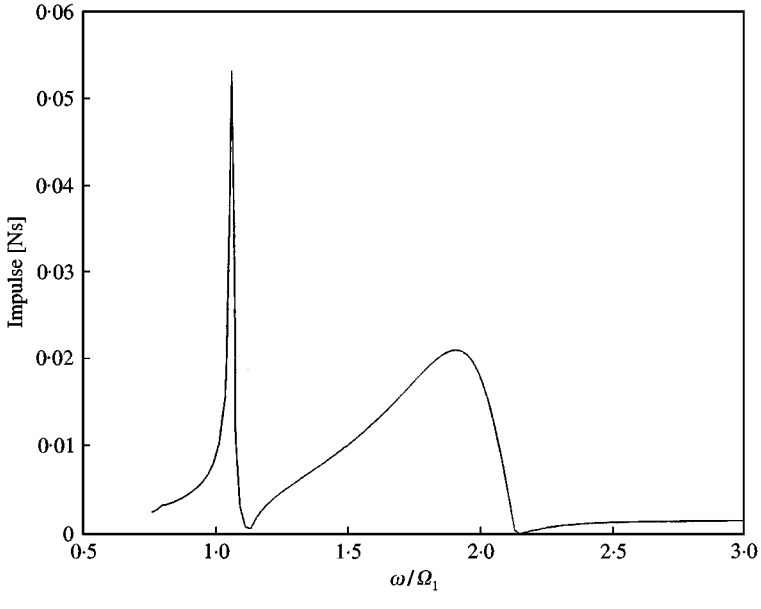

Figure 8. Frequency response of J to impact excitation.

6. COMPARISON WITH NUMERICAL SIMULATION

The PGF results shown in the previous section can be compared with a numerical simulation carried out in SIMULINK. To bring the problem close to

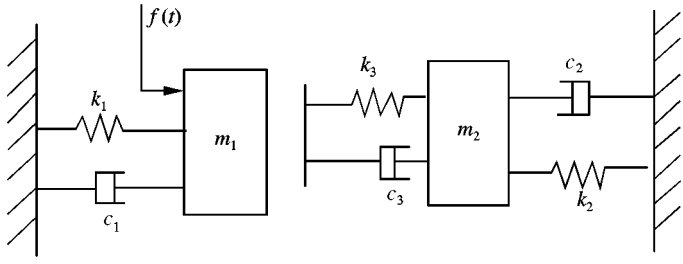

Figure 9. Model with compliance used in Simulink studies

reality the model was altered to include a compliance between the two masses. The type of compliance chosen was a viscoelastic model containing a spring and damper (see Figure 9), as proposed in reference [18]. As the laboratory model consisted of two steel masses, the stiffness was set at a high value ($k_3 = 100\,000$ N/m) and the damping at a low value ($c_3 = 0{\cdot}1$ Ns/m). The simulation model detects when the contact between the two masses has occurs and brings the compliance into operation. Once the masses start to move apart the simulation monitors the forces acting on the masses due to the compliance, and when these sum to zero the simulation turns the compliance off. The alternative method of switching off the compliance after a particular distance can cause a physically impossible tensile force in the compliant surface.

Two types of excitation were applied to this model, one was sinusoidal and the other was a series of narrow pulses representing impact excitation. The same parameters as those used for the PGF model were used, except that $c_1 = c_2 = 0{\cdot}1$ Ns/m and the magnitudes of the excitations required a little adjustment to create vibro-impact behaviour.

With sinusoidal excitation, the r.m.s. displacement behaviour of the model with a compliant surface is shown in Figures 10 and 11. When the frequency is swept up through the resonances, both resonances are excited and they are at 5·7 and 10·6 Hz, Figure 10(a) shows the result for m_1 and Figure 10(b) the result for m_2. Notice that the first resonance has no frequency pulling while the second resonance clearly demonstrates frequency pulling and jump effects. As with the PGF results, the first resonance is a grazing resonance and the second is a clapping resonance. When the frequency of excitation is swept down through the resonances, only the first resonance is excited (Figure 11(a) and (b)). Figure 12 shows the reaction force Q of the compliant surface against the frequency for the unsweep. This reaction force is related to J the impulse between the two surfaces and shows some similarly to the graph of J (Figure 8) calculated in the previous section.

The results from the model when pulse excitation is applied are almost similar, so only the displacement results (for both masses) for the unsweep are presented here (see Figure 13(a) and (b)). The resonances are at 5·7 and 10·7 Hz. Again the first resonance is a grazing resonance and is excited on both the unsweep and downsweep. The second resonance is a clapping resonance and is only excited on the upsweep of the excitation frequencies. The additional small peak in

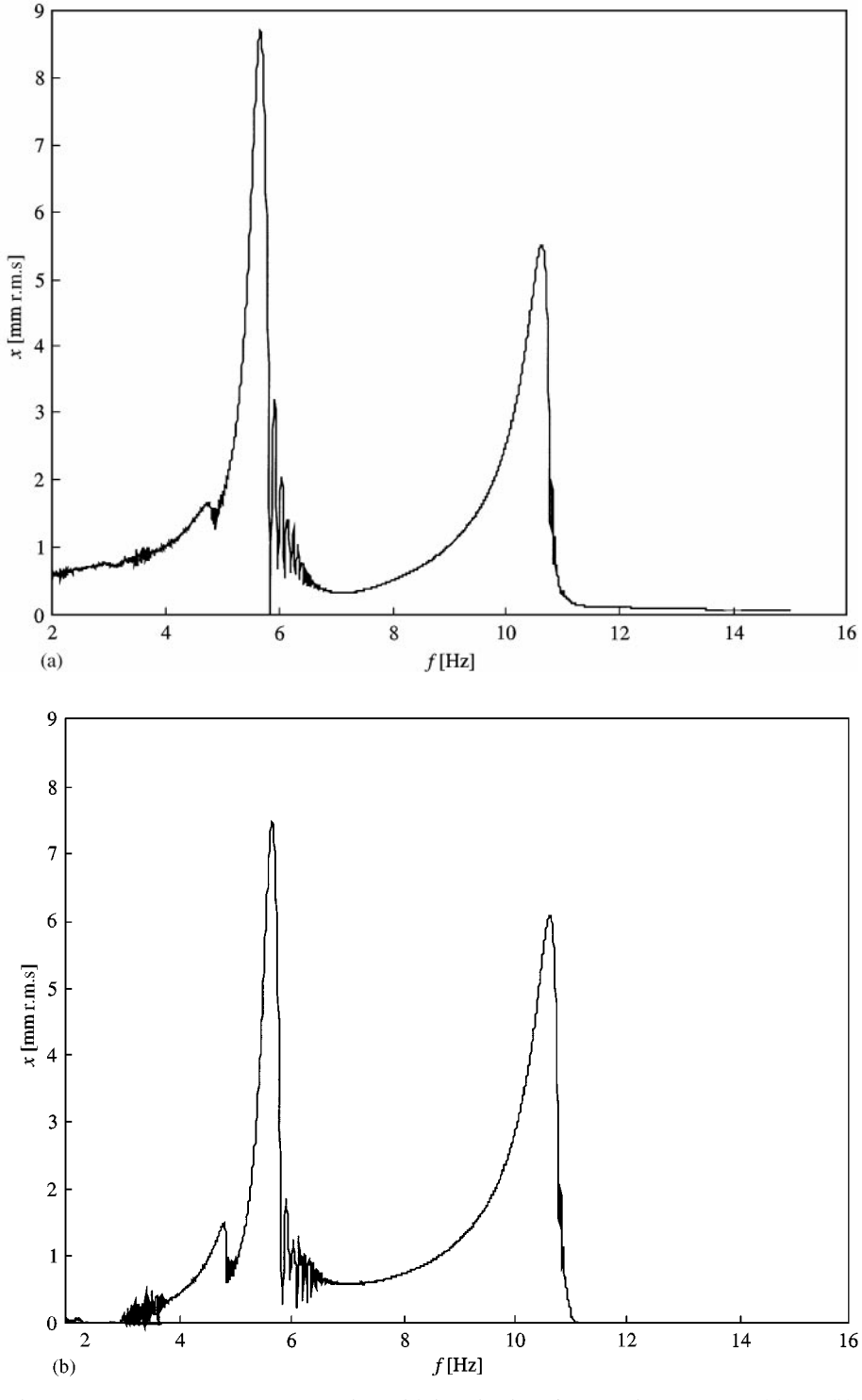

Figure 10. Frequency response to sinusoidal excitation, frequencies swept up (a) x_1, (b) x_2.

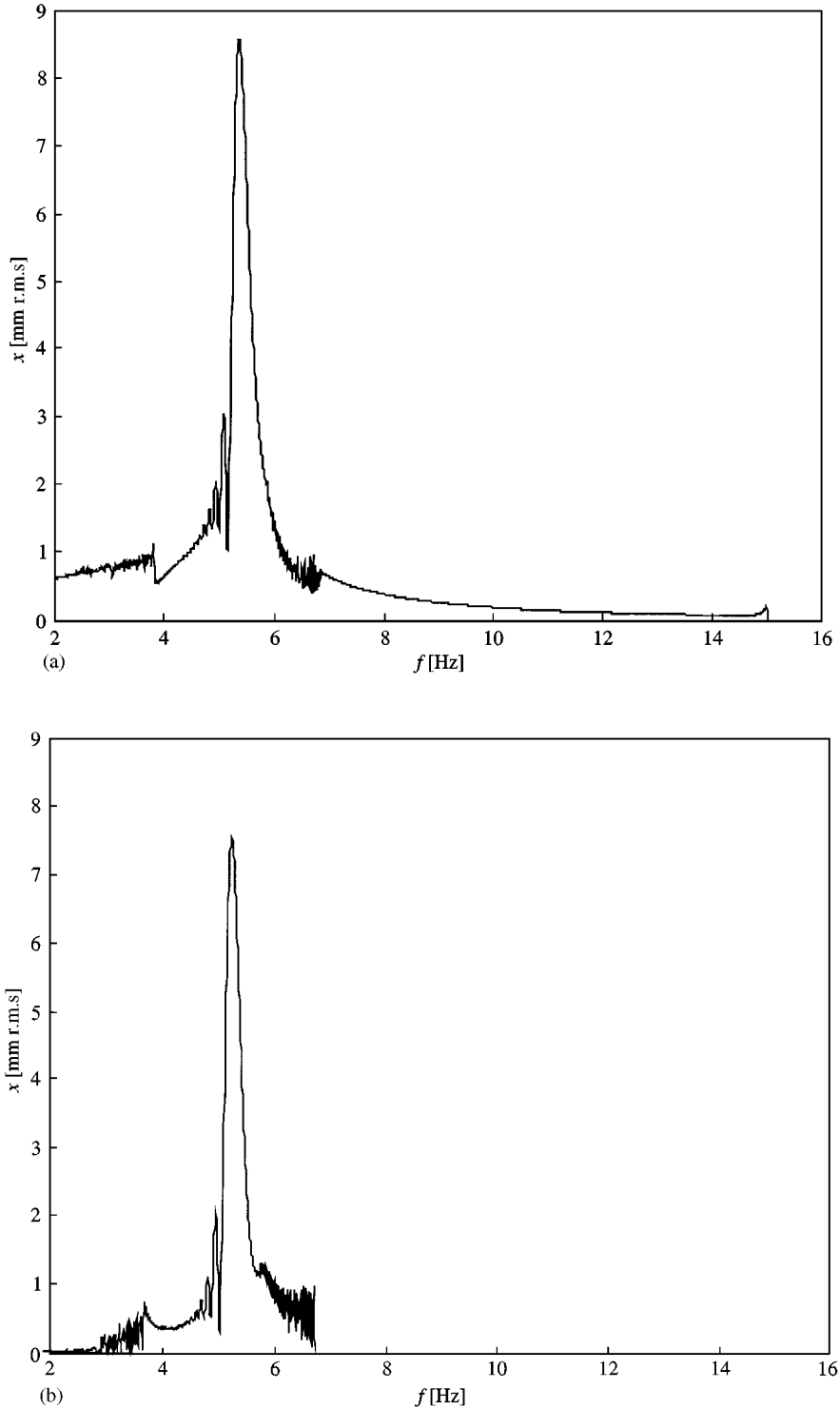

Figure 11. Frequency response to sinusoidal excitation, frequencies swept down (a) x_1, (b) x_2.

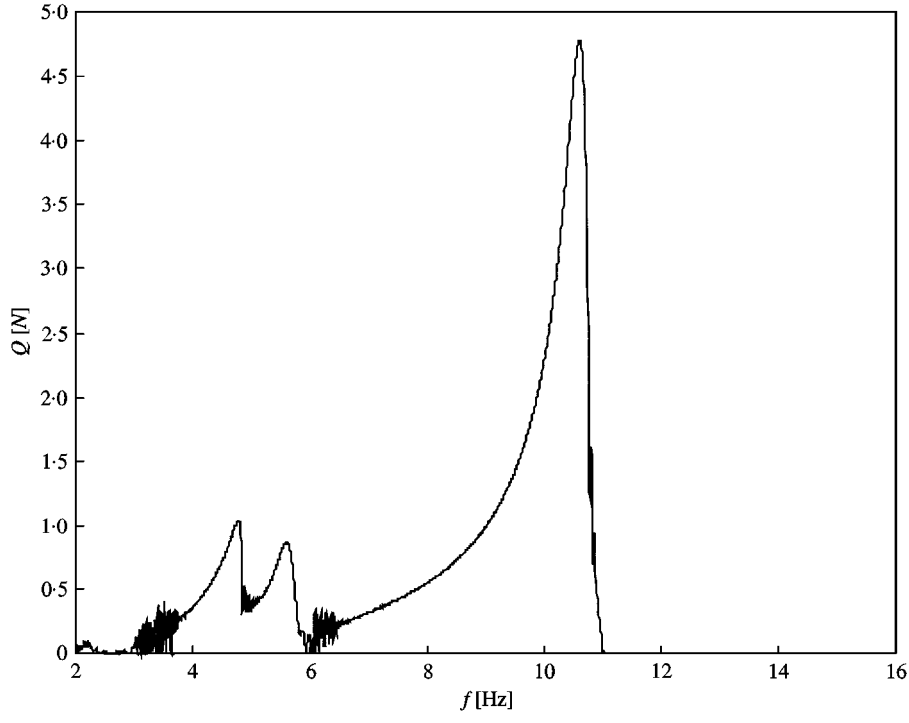

Figure 12. Frequency response to reaction force to sinusoidal excitation, frequenies swept up.

low-frequency range is a super-periodic resonance typical for the use of pulse excitation. The simulation results are in good agreement with the experiment and the PGF method, as regards both the frequencies and the overall behaviour of the system.

7. CONCLUSIONS

It has been demonstrated that the periodic Green function method is capable of analytically solving the equation of motion of a two-degree-of-freedom vibro-impact system with periodic impulse excitation. The overall behaviour and resonance frequencies predicted by the technique are in good agreement with the laboratory measurements carried out. Further work is required to produce a rigorous proof of solution stability. The PGF method may be applied to a variety of vibro-impact systems and the model used here could be extended to more complex problems. This could also include real systems whose mathematical descriptions are limited to experimental data collected at a few physically accessible points.

The results from the PGF method have provided a solid basis for the computer-based simulation so that more complex systems can be safely modelled in Simulink without the uncertainty of possible numerical integration errors. However, are detailed comparisons could be carried out on the current model

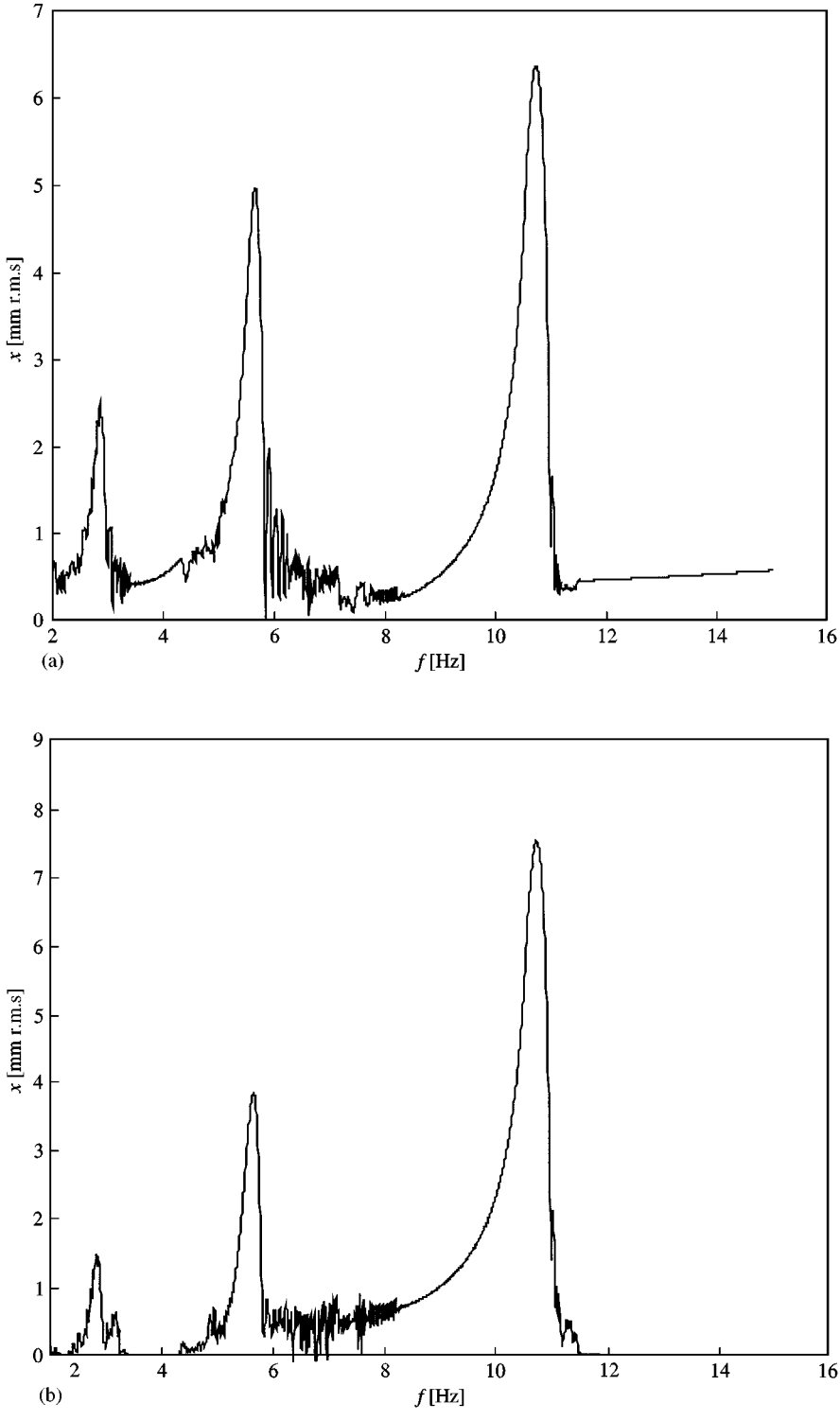

Figure 13. Frequency response to pulse excitation, frequencies swept up (a) x_1, (b) x_2.

between the PGF method, computer-based simulations and experiment especially as regards the amplitude levels.

ACKNOWLEDGMENT

The authors would like to thank Dr A. Veprik for advice given on Simulink and compliant surfaces, and the Engineering and Physical Sciences Research Council for funding the research under which this study was carried out.

REFERENCES

1. A. I. Lurie 1951 *Operational Calculus*. Moscow: Gostekhtheorizdat, second edition (in Russian).
2. I. G. Rusakov and A. A. Kharkevich 1942 *Journal of Technical Physics* **12**, 715–721. Forced vibrations of a system that is striking a stop (in Russian).
3. R. E. Brunstein, A. E. Kobrinskii 1969 Chapter 7–9 In: A. E. Kobrinskii *Dynamics of Mechanisms with Elastic Connections and Impact Systems*, London: Iliffe Books, (translation from Russian edition, Moscow: Nauka, 1964).
4. L. V. Bespalova, Yu. I. Neimark, M. I. Feigin 1966 *Engineering Journal Mechanics of Solids* **1**, 151–159. Dynamical systems with impact interactions and the theory of nonlinear oscillations (in Russian).
5. V. I. Babitsky 1978 *Theory of Vibro-Impact Systems*. Moscow: Nauka, (Revised English translation from Russian: 1998 Berlin, Heidelbnerg, New York: Springer.)
6. V. I. Babitsky, M. Z. Kolovsky 1976 *Mechanics of Solids* **4**, 88–91. To investigation of resonances in vibro-impact systems (in Russian).
7. E. I. Jury 1958 *Sampled-Data Control Systems*. New York: Wiley.
8. E. N. Rosenwasser 1969 *Vibrations of Nonlinear Systems*. Moscow: Nauka (in Russian).
9. C. Grubin 1956 *Journal of Applied Mechanics* **23**. On the theory of the acceleration damper.
10. R. N. Arnold 1957 *Actes IX Congress on Applied Mechanics, Brussels*. Response of an impact vibration absorber to forced vibration.
11. V. I. Babitsky, V. L. Krupenin 1985 *Vibrations in Strongly Nonlinear Systems*. Moscow: Nauka (in Russian).
12. A. S. Kovaleva 1990 *Control of Vibrating and Vibro-Impact Systems*. Moscow: Nauka (English translation from Russian: Optimal Control of Mechanical Oscillations 1999 Berlin, Heidelberg, New York: Springer).
13. A. M. Veprik, V. L. Krupenin 1988 *Machine sciences* **6**, 39–47. On the resonance oscillation of a system with a distributed impact element (in Russian).
14. W. H. Park 1967 *Journal of Engineering for Industry, Transactions of the ASME* **89**, 587–596. Mass–spring–damper response to repetitive impact.
15. Cz. Cempel 1971 *Engineering Reports* **19**, 301–307. The percussive vibration of two independent systems (in Polish).
16. T. Irie, K. Fukaya 1972 *Bulletin of the JSME* **15**, 299–306. On the stationary impact vibration of a mechanical system with two degrees of freedom.
17. F. Peterka, O. Szollos 1996 *EUROMECH 2nd European Nonlinear Oscillation Conference, Prague, Vol* 1, The stability analysis of a symmetric two-degree-of-freedom system with impacts.
18. V. I. Babitsky, A. M. Veprik 1998 *Journal of Sound and Vibration* **218**, 269–292. Universal bumpered vibration isolator for severe environment.
19. D. J. Ewins 1984 *Modal Testing: Theory and Practice*, Taunton: Research Studies Press.

20. L. MEIROVITCH 1986 *Elements of Vibration Analysis*. New York: McGraw-Hill, second edition.
21. L. SCHWARTZ 1961 *Méthodes Mathématiques pour les Sciences Physiques*. Paris: Hermann.

APPENDIX: THE PERIODIC GREENS FUNCTION OR A SINGLE-DEGREE-OF-FREEDOM SYSTEM

This section develops a periodic Green function for the system shown in Figure A1. The mathematical description of such functions as impulse–frequency characteristics and their use in general non-linear analysis has been published in reference [8]. In reference [11] and in the later work on their applications in analysis of mechanical systems they became known as periodic Green functions.

The equation of motion for damped vibration for a single-degree-of-freedom system is

$$m\ddot{x} + c\dot{x} + kx = f(t). \tag{A1}$$

If the excitation is $f(t) = Qe^{i\omega t}$ assume the periodic solution is $x(t) = X(i\omega)e^{i\omega t}$ (where $X(i\omega)$ is a complex amplitude) then the equation of motion becomes

$$(m(i\omega)^2 + ci\omega + k)X(i\omega)e^{i\omega t} = Qe^{i\omega t}. \tag{A2}$$

So the dynamic compliance (ratio between the complex amplitudes of steady state displacement and force) is

$$L(i\omega) = \frac{1}{(k - \omega^2 m) + i(\omega c)} = \frac{X(i\omega)}{Q}. \tag{A3}$$

The dynamic compliance gives a measure of the response of the system to a periodic excitation and it can be rewritten in the form

$$L(i\omega) = \frac{1}{m(\Omega^2 + (i\omega)^2 + 2bi\omega)}. \tag{A4}$$

where $\Omega^2 = k/m$, $2b = 2\Omega\zeta = c/m$ and Ω is the undamped natural frequency of the fundamental mode and ζ is the damping ratio. The derivation of the dynamic compliance can be found in a number of books on vibration [19, 20].

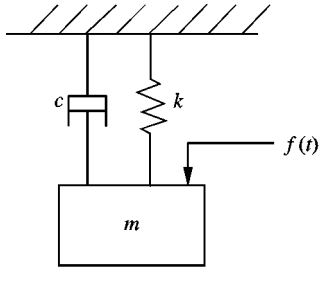

Figure A1. Single-degree-of-freedom system.

A periodic impulse excitation can be represented by a periodic series of Dirac δ functions:

$$f(t) = \sum_{v=-\infty}^{\infty} \delta(t - vT), \tag{A5}$$

where T is the time between the pulses. The excitation $f(t)$ can also be written as a Fourier series [21]:

$$f(t) = \frac{1}{T} \sum_{n=-\infty}^{\infty} e^{in\omega t},$$

where $\omega = 2\pi/T$. (A6)

The steady state response due to the series of impulses can then be written as

$$\chi(t) = \frac{1}{T} \sum_{n=-\infty}^{\infty} L(ni\omega) e^{ni\omega t} \tag{A7}$$

which is the periodic Green function.

Substituting equation (A4) into equation (A7) gives

$$\chi(t) = \frac{1}{Tm} \sum_{n=-\infty}^{\infty} \frac{1}{\Omega^2 + (ni\omega)^2 + 2b(ni\omega)} e^{ni\omega t}. \tag{A8}$$

Series (A8) gives the steady state response of the system to a sequence of impulses at $t = \ldots -3T, -2T, -T, 0, T, 2T, 3T \ldots$. It can be transformed into a finite expression as follows to cover just one period by using a formula provided in reference [8].

A generalized PGF takes the form

$$\chi(t) = \frac{1}{T} \sum_{n=-\infty}^{\infty} L(ni\omega)\, e^{ni\omega t}. \tag{A9}$$

If the polynomial $L(ni\omega)$ has the fractional-rational structurre

$$L(p) = \frac{m(p)}{d(p)} = \frac{m_0 p^{2k-2} + m_1 p^{2k-3} + \cdots + m_{2k-2}}{d_0 p^{2k} + d_1 p^{2k-1} + \cdots + d_{2k}} \tag{A10}$$

and the roots of the equation $d(ni\omega) = 0$ are simple (all different), then the PGF (equation (A9)) can be rewritten as

$$\chi(t) = \sum_{\rho=1}^{n} \frac{m(p_\rho)}{d'(p_\rho)} \frac{e^{p_\rho t}}{1 - e^{p_\rho T}}, \quad 0 < t < T, \tag{A11}$$

where p_ρ are the roots of the equation $d(ni\omega) = 0$ and $'$ indicates a differentiated variable. So equation (A8) becomes

$$\chi(t) = \frac{1}{m} \sum_{\rho=1}^{n} \frac{1}{2p_\rho + 2b} \frac{e^{p_\rho t}}{1 - e^{p_\rho T}}, \quad 0 < t < T. \tag{A12}$$

The roots of the equation $d(ni\omega) = 0$ are $p_{1,2} = -b \pm i\sqrt{\Omega^2 - b^2}$. Substituting these two roots into (A12) gives

$$\chi(t) = \frac{1}{m}\left(\frac{1}{2(-b + i\lambda) + 2b}\frac{e^{-bt}e^{i\lambda t}}{1 - e^{-bT}e^{i\lambda T}}\right) + \frac{1}{m}\left(\frac{1}{2(-b - i\lambda) + 2b}\frac{e^{-bt}e^{-i\lambda t}}{1 - e^{-bT}e^{-i\lambda T}}\right),$$

where $\lambda = \sqrt{\Omega^2 - b^2}$. After rearranging, it follows that

$$\chi(t) = \frac{e^{-bt}}{2im\lambda}\left(\frac{e^{i\lambda t}}{1 - e^{-bT}e^{i\lambda T}} - \frac{e^{-i\lambda t}}{1 - e^{-bT}e^{-i\lambda T}}\right), \quad 0 < t < T \tag{A13}$$

As $e^{i\theta} = \cos\theta + i\sin\theta$, equation (13) becomes

$$\chi(t) = \frac{e^{-bt}}{m\lambda}\left(\frac{\sin\lambda t + e^{-bT}\sin\lambda(T - t)}{1 + e^{-2bT} - 2e^{-bT}\cos\lambda T}\right), \quad (0 < t < T) \tag{A14}$$

Equation (A14) represents the periodic Green function (PGF) over one period for a single-degree-of-freedom system. Note that this PGF reflects the steady state periodic behaviour of the system with one impact per cycle occuring at $t = 0$ (impact also occurs $t = T$ which is the beginning of the next period).

If there is a time lead τ, where $0 < \tau < T$ (impact does not occur at $t = 0$), it is possible to write the PGF as

$$\chi(t + \tau) = \frac{1}{T}\sum_{k=-\infty}^{\infty}\frac{m(ki\omega)}{d(ki\omega)}e^{ki\omega(t+\tau)}. \tag{A15}$$

In reference [8] a transformation is given for a PGF with time lag where the result is not one equation but two, so that the term $t - \tau$ is kept within the range of one period as long as τ is less than one period T. By analogy, a similar pair of equations can be set up for a PGF with time lead as follows:

$$\chi(t + \tau) = \left\{\begin{array}{ll} \displaystyle\sum_{\rho=1}^{n}\frac{m(p_\rho)}{d'(p_\rho)}\frac{e^{p_\rho(t+\tau-T)}}{1 - e^{p_\rho T}}, & 0 < t < T \text{ and } T < t + \tau < 2T \\ \displaystyle\sum_{\rho=1}^{n}\frac{m(p_\rho)}{d'(p_\rho)}\frac{e^{p_\rho(t+\tau-T)}}{1 - e^{p_\rho T}}, & 0 < t < T \text{ and } 0 < t + \tau < T \end{array}\right\}, \tag{A16}$$

Other PGFs can be calculated for more complicated systems and systems with more than one impact per cycle. A non-linear oscillator may require linearizing before creating a PGF. Also a PGF can be developed from a dynamic compliance of an analyzed system which has been measured experimentally.